HHS Public Access

Author manuscript

*J Mol Cell Cardiol*. Author manuscript; available in PMC 2016 November 01.

Published in final edited form as:

*J Mol Cell Cardiol*. 2015 November ; 88: 1–13. doi:10.1016/j.yjmcc.2015.09.004.

# Cardiomyocyte-Specific Overexpression of the Ubiquitin Ligase Wwp1 Contributes to Reduction in Connexin 43 and Arrhythmogenesis

**Wassim A. Basheer**[a], **Brett S. Harris**[b], **Heather L. Mentrup**[a], **Measho Abreha**[a], **Elizabeth L. Thames**[a], **Jessica B. Lea**[a], **Deborah A. Swing**[c], **Neal G. Copeland**[c,1], **Nancy A. Jenkins**[c,1], **Robert L. Price**[d], and **Lydia E. Matesic, Ph.D.**[a,2]

[a]Department of Biological Sciences, University of South Carolina, Columbia, SC 29208, USA

[b]Department of Regenerative Medicine and Cell Biology, Medical University of South Carolina, Charleston, SC 29425, USA

[c]Mouse Cancer Genetics Program, The National Cancer Institute at Frederick, Frederick, MD 21702, USA

[d]Department of Cell Biology and Anatomy, University of South Carolina School of Medicine, Columbia, SC 29209, USA

## Abstract

Gap junctions (GJ) are intercellular channels composed of connexin subunits that play a critical role in a diverse number of cellular processes in all tissue types. In the heart, GJs mediate electrical coupling between cardiomyocytes and display mislocalization and/or downregulation in cardiac disease (a process known as GJ remodeling), producing an arrhythmogenic substrate. The main constituent of GJs in the ventricular myocardium is connexin 43 (Cx43), an integral membrane protein that is rapidly turned over and shows decreased expression or function with age. We hypothesized that Wwp1, an ubiquitin ligase whose expression in known to increase in aging-related pathologies, may regulate Cx43 *in vivo* by targeting it for ubiquitylation and degradation and yield tissue-specific Cx43 loss of function phenotypes. When Wwp1 was globally overexpressed in mice under the control of a β-actin promoter, the highest induction of *Wwp1* expression was observed in the heart which was associated with a 90% reduction in cardiac Cx43 protein levels, left ventricular hypertrophy (LVH), and the development of lethal ventricular arrhythmias around 8 weeks of age. This phenotype was completely penetrant in two independent founder lines. Cardiomyocyte-specific overexpression of Wwp1 confirmed that this phenotype was cell autonomous and delineated Cx43-dependent and –independent roles for Wwp1 in

[2]To whom correspondence should be addressed: 715 Sumter St., Columbia, SC 29208 USA (lmatesic@biol.sc.edu), Phone (803) 777-2520, FAX (803) 777-4002.

[1]Present Address: The Methodist Cancer Research Program, The Methodist Hospital Research Institute, Houston, TX 77030, USA



**Disclosures**

None.

arrhythmogenesis and LVH, respectively. Using a cell-based system, it was determined that Wwp1 co-immunoprecipitates with and ubiquitylates Cx43, causing a decrease in the steady state levels of Cx43 protein. These findings offer new mechanistic insights into the regulation of Cx43 which may be exploitable in various gap junctionopathies.

**Keywords**

Connexin; gap junction; Wwp1; ubiquitin; arrhythmogenesis

## 1. Introduction

Gap junctions (GJ) play an instrumental role in the electrical coupling of cardiomyocytes and, consequently, in synchronization of myocardial contraction. Connexin 43 (Cx43) is the principle constituent of GJs in the working mammalian myocardium, and decreases in Cx43 expression and/or altered subcellular localization of Cx43 (a process termed GJ remodeling) have been described in nearly every type of cardiac pathology, including aging [1], and correlate with electrophysiologically identified arrhythmic changes and contractile dysfunction in animal models [2]. Indeed, mounting evidence supports the assertion that arrhythmogenesis resulting from GJ remodeling is the common endpoint of a myriad of different etiologies, both acquired and genetic [3]. Therefore, there is great interest in understanding the molecular pathways that regulate both normal GJ homeostasis as well as those involved in pathological GJ remodeling.

GJ plaques are dynamic plasma membrane domains that are constantly being renewed and degraded. Cx43 is an unusually labile integral membrane protein with an estimated half-life in the heart of less than two hours [4–6]. Ubiquitylation of Cx43 or associated proteins is an important cellular signal in its physiological internalization and degradation [7, 8], and recently it has been found that Cx43 is also ubiquitylated in cultured cardiomyocytes that undergo ischemia [9, 10]. Ubiquitylation is a post-translational modification that covalently conjugates the highly conserved ubiquitin (Ub) molecule via its C-terminus to a lysine residue on a target protein. This signal can result in the turnover of the ubiquitylated substrate by either the proteasome or by the lysosome, a change in subcellular localization of the target protein, or alteration of target protein function [11]. This process is facilitated by three enzymes/scaffolding proteins: the Ub-activating enzyme (E1), the Ub-conjugating enzyme (E2), and the Ub ligase (E3). Because there are only a limited number of E1s and a handful of E2s, much of the specificity in ubiquitylation is thought to be determined by the E3 [12].

Several reports show that a growing number of E3s can regulate Cx43 and its internalization from the plasma membrane, including TRIM21 [13], Smurf2 [14], and Nedd4 [15, 16]. Since these studies were conducted in cell culture systems, the issue of how Cx43 degradation may be regulated *in vivo* is still unclear. We hypothesized that the E3 ubiquitin ligase Wwp1 may contribute to the regulation of Cx43 levels in the heart and, potentially, to GJ remodeling as well. Wwp1 shares overall structural organization with Nedd4 and Smurf2, including a phospholipid-associated C2 domain, 4 WW domains which have

affinity for PY motifs and phospho-serines and -threonines, such as those found in the carboxy terminus of Cx43, as well as the enzymatic HECT domain [17]. Furthermore, high expression of *WWP1* in the heart has been reported [18–20], suggesting that it may have an important physiological function there. Dysfunction of WWP1 has been implicated in tumorigenesis, neurological disorders, infectious disease responses, and in aging [21]. Specifically, somatic genomic amplification or overexpression of *WWP1* has been associated with the development of a variety of cancers [22–26], and the mechanism underlying its oncogenic effects commonly involves the ubiquitylation of tumor suppressors [21]. WWP1 expression has also been reported to increase in mouse mesenchymal stem cells with age, whereas *Wwp1*$^{-/-}$ mice exhibited increased bone mass due to increased osteoblast migration, differentiation, and function [27]. Thus, WWP1 appears to have an important role in bone homeostasis which is disrupted in aging with the appearance of osteoblast dysfunction and bone loss. Since mice lacking Cx43 have low bone mass and osteoblast dysfunction [28], humans with mutations in the *GJA1* gene encoding Cx43 develop skeletal malformations and infrequent cardiac abnormalities like arrhythmias as part of the syndrome oculodentodigital dysplasia (ODDD) [29], and Cx43 has been characterized as a conditional tumor suppressor [30], we considered the possibility that Wwp1 may negatively regulate Cx43 *in vivo*.

Using an inducible transgenic mouse model, we herein demonstrate a novel role for Wwp1 in the regulation of Cx43 in the heart. In two independent founder lines, β-actin-induced global activation of the transgene resulted in the highest level of induction of Wwp1 expression in the heart which was associated with a ~90% reduction of steady state levels of myocardial Cx43 protein levels, left ventricular hypertrophy (LVH), and the development of lethal ventricular arrhythmias between 5 and 13 weeks of age with 100% penetrance. Cardiomyocyte-specific overexpression of Wwp1 confirmed that this phenotype was cell autonomous and delineated Cx43-dependent and –independent roles for Wwp1 in arrhythmogenesis and LVH, respectively. These findings offer new mechanistic insights into the regulation of Cx43 which may be exploitable in various gap junctionopathies from arrhythmogenesis to carcinogenesis.

## 2. Materials and methods

### 2.1. Animals

The pTraffic transgenic vector was created by ligating an 8.2 kb SacI/EcoRV fragment from pRedInC (provided by Dr. Adam Dupuy, University of Iowa School of Medicine) with a double stranded oligo of the sense sequence 5’-CGGCGCGCCATCGATGCTAGCGATATCGCATGCTCGA-3’, and a 1.3 kb BamHI/BsaBI fragment from pIRES2-eGFP (Clontech). The full length 2756 bp open reading frame of Wwp1 was then directionally cloned into the AscI and NheI sites of the polylinker. To generate pTraffic-Wwp1 mice, the PvuI-linearized construct into fertilized pronuclei from C57BL/6N zygotes. Founder animals were identified by DsRed2 expression and confirmed by Southern blot analysis and used to create lines on a C57BL/6N background. These were bred to homozygous beta-actin cre animals (FVB/N-Tg(ACTB-cre) 2Mrt/J, Jackson stock number 003376) to generate global Wwp1 overexpressers (tg/+; cre/+). To generate

cardiomyocyte-specific overexpressers, pTraffic-Wwp1 transgenics were crossed to animals homozygous for the Tmx-inducible MerCreMer transgene (B6.FVB(129)-Tg(Myh6-cre/Esr1*)1Jmk/J, Jackson stock number 005657) and resulting tg/+; MerCreMer/+ were injected with Tamoxifen base (T5648, Sigma-Aldrich) resuspended in a 95% peanut oil (P2144, Sigma–Aldrich) 5% ethanol solution to induce Wwp1 overexpression. The dosing regime was two consecutive dosages of 40 mg/kg/day spaced by 24 hours as previously described in [31]. All experiments were conducted in full compliance with the Institutional Animal Care and Use Committee of the University of South Carolina, the Medical University of South Carolina, and the National Cancer Institute at Frederick.

### 2.2. Quantitative real time PCR

Following erythrocyte lysis, $CD45^+$ and $CD45^-$ cells were obtained from mouse bone marrow using CD45 MicroBeads and LD columns in accordance with the manufacturer's instructions (Miltenyi Biotec). Total RNA was isolated from mouse tissues using RNA STAT-60 (Tel-Test) following the specifications provided by the manufacturer. One microgram of total RNA was used in cDNA synthesis primed with random hexamers using the Roche Reverse Transcription kit. Quantitative real time PCR reactions were performed in triplicates in a 96-well plate (Applied Biosystems) using the 7300 Real-Time PCR System (Applied Biosystems) with SYBR Green PCR Master Mix (Applied Biosystems). All reactions were run at 50° C for 2 min, then 95°C for 10 minutes, then 40 cycles of 95°C for 15 seconds and 60°C for 1 minute. A melting curve analysis was added after each run to confirm the specificity of the amplification (95°C for 15 sec, then 60°C for 30 sec followed by 95°C for 15 sec). *Gapdh* was used as reference gene and the relative expression was calculated as in [32]. Primer sequences used in this analysis were as follows: 5'-GCTTCCAGGCCATATTGGAG-3' and 5'-GGGGGCATGACCTCATCTT-3' for *Nppb*, 5'-GAGGTCACTCCTATCCTCTGG-3' and 5'-GCCATTTCCTCCGACTTTTCTC-3' for *Nppa*, 5'-ACAACCCCTACGATTATGCGT-3' and 5'-ACGTCAAAGGCACTATCCGTG-3' for *Myh7*, 5'-GGCAGTCTCAGCGGAATCAAT-3' and 5'-GGTCCATAGGGGTCATTTTCTG-3' for *Wwp1*, 5'-AGAACACGGCAAGGTGAAGAT-3' and 5'-TGAACCCATAGATGTACCACTGG-3' for *Cx43*, and 5'-TGAAGCAGGCATCTGAGGG-3' and 5'-CGAAGGTGGAAGAGTGGGAG-3' for *Gapdh*.

### 2.3. Cardiomyocyte cross sectional area

90 μm vibratome cardiac sections were stained with TRITC-conjugated wheat germ agglutinin (WGA, Sigma) and DAPI. The images were acquired using an IX81 Olympus spinning disk confocal microscope at 20X oil magnification. The surface area and diameter of 250 cardiomyocytes from 15 different fields (in cross section) per animal were measured by an observer blind to genotype using ImageJ.

### 2.4. Echocardiography

Transthoracic echocardiography imaging was performed on anesthetized animals using a VEVO 660 ultrasound machine with a 25-MHz RMV-710 transducer. The heart was first imaged in a two-dimensional mode (B mode) in the parasternal short-axis view and then this

view was used to position the M-mode cursor perpendicular to the ventricular septum and LV posterior wall, after which one-dimersional M-mode echocardiogram traces were obtained and analyzed. All primary measurements were made from images captured on cine loops at the time of the study by use of the instrument-based VisualSonics analysis software present. For each study, measurements were made and averaged from 9 heart beats per animal.

### 2.5. Electrocardiograms

Three lead surface electrocardiograms were obtained on lightly anesthetized mice. Electrogram signals were amplified and filtered using a BioAmp (ADInstruments) and acquired at 1–2 kHz using a PowerLab 8/35 (ADInstruments). Electrocardiograms were analyzed and measurements of cardiac intervals from at least 10 waveforms of each recording were made using LabChart (ADInstruments).

### 2.6. Overdrive pacing

Mouse hearts were isolated and cannulated via the aorta and Langendorff perfused with Tyrode solution (pH=7.4). Tyrode solution was saturated with 100% oxygen and maintained at 37°C. A second cannula was inserted via the pulmonary vein, through the left atrium and across the mitral valve. Hearts were placed in a tissue bath mounted on a THT microscope (Scimedia) and positioned with the posterior side down such that anterior free wall (frontal four chamber view) could be imaged and a stable ventricular rhythm established. To pace the ventricles, bipolar 22G Teflon coated chloride-silver wire electrodes were positioned at the AV groove. Three additional monopolar electrodes were positioned on the ventricular free wall to record ventricular epicardial electrocardiograms. Stimulation pulses were at a duration of 2 ms and an amplitude of twice threshold. The overdrive pacing protocol consisted of a burst of 20 pulses over a short 1.5 s time period (equivalent to a heart rate of 750 bpm). To record high resolution 1 kHz electrocardiograms, signals were amplified and filtered by an electrocardiogram amplifier at a bandwidth of 0.1 to 300 Hz (WPI) using a Bioamp (BD Instruments), captured, and analyzed using Labchart software. All recordings were obtained simultaneously throughout the duration of the pacing protocols.

### 2.7. Tissue Immunofluorescence

Mouse cardiac tissue was flash frozen in freezing medium (Thermo Scientific), and cryosectioned at 10 μm. Sections were fixed in 2% PFA and blocked in 10% normal donkey serum, 2% BSA and 0.2% Triton X-100 in TBS. Primary antibody was applied in 1% normal donkey serum/0.1% Triton X-100 in TBS and incubated overnight at 4°C. Primary antibodies used include Cx43 (C6219, Sigma, 1:500), N-Cadherin (3B9, Invitrogen, 1:500), and desmoplakin1/2 (DP-2.15, AbD Serotec, 1:50). The appropriate Cy3- or Cy5-conjugated secondary antibody (Jackson ImmunoResearch) was applied at a 1:200 dilution (in 1% normal donkey serum and 0.1% Triton X-100 in TBS) and then phalloidin was detected using 1x blue 350-phalloidin (AAT Bioquest). All images were acquired using an IX81 Olympus spinning disk confocal microscope at 60X oil magnification and sometimes pseudocolored for figure production.

Paraffin sections of normal human heart or left ventricle were purchased from Biomax and Biochain, respectively, The slides were dewaxed, treated with antigen retrieval solution (DAKO), permeabilized with Triton X-100, blocked for one hour using donkey antiserum followed by incubation with primary antibodies (Cx43, C6219, Sigma, 1:4000 and Wwp1, 1A7, Abnova, 1:1000) overnight. The slides were washed with phosphate buffered saline and incubated with the appropriate Cy2- or Cy3-conjugated secondary antibody (Jackson ImmunoResearch) for one hour. Images were acquired using a Zeiss Axioimager A1 at 40X.

### 2.8. Tissue Protein Extraction and Western Blot Analysis

Mouse hearts were quickly dissected out following euthanasia and immediately homogenized in 1 mL of freshly prepared protein lysis buffer (50 mM Tris pH=8, 150 mM NaCl, 1% Triton X-100, 1 mM DTT, 25mM NaF, 10 mM of freshly made iodoacetamide, 2mM of sodium orthovanadate, 1X EDTA and protease cocktail inhibitors from Thermo Scientific). The protein lysates were incubated on ice for 30 min then centrifuged for 30 min at 14,000 rpm (4°C). For western blotting, 50 μg or 100 μg of protein per sample were separated using a 10% or 4%-20% gradient Bio-Rad Criterion TGX Tris-Glycine Gels then transferred to a PVDF membrane. Signals were visualized using ECL reagent (Millipore, Immobilon Western) and the FluorChem E Chemiluminescent Western Blot Imaging System (ProteinSimple). Normalization and quantification of band intensities was performed with AlphaView software (ProteinSimple). Primary antibodies used include anti-RFP/DsRed2 (ab62341, Abcam, 1:1000), anti-eGFP (ab290, Abcam, 1:2000), anti-Cx43 (C6219, Sigma, 1:1000 or 1:4000 in ubiquitylation assay), anti-HA (H9658, Sigma, 1:4000), anti-MYC (9E10, Santa Cruz Biotechnology, 1:500), anti-Cx40 antiserum (Alpha Diagnostic International, 1:1000), anti-Cx45 (AB1745, Millipore, 1:1000), and anti-α-Tubulin (T5168, Sigma, 1:1000). HRP-conjugated secondary antibodies were from BioRad and Santa Cruz Biotechnology.

### 2.9. Co-immunoprecipitation

293T cells were transfected with 2 μg total of the indicated plasmids using JetPRIME reagent (PolyPLUS) according to the manufacturer's guidelines. Forty-eight hours after transfection, cells were stimulated with 100 ng/mL of phorbol 12-myristate 13-acetate (PMA) for 30 min, the PMA was washed out, and the cells were lysed 5.5 hours later with a solution containing 50 mM Tris-HCl, pH 7.4, 150 mM NaCl, 0.5% Triton X-100, 2.5 mM EDTA, 2 mM sodium orthovanadate, 10 mM iodoacetamide, and protease cocktail inhibitors (Thermo Scientific). After reserving 3.75% of the cell lysate to run as input, the remainder was pre-cleared with protein A/G agarose beads (Santa Cruz Biotechnology) and then incubated with 1 μg of either anti-Cx43 (71–0700, Invitrogen) antibody or control anti-rabbit IgG overnight. The next day, the immunocomplexes were incubated with protein A/G agarose beads (Santa Cruz Biotechnology) for three hours, washed in lysis buffer, eluted with 2X Laemmli sample buffer after boiling for 5 min at 95°C, resolved using SDS-PAGE, and blotted with the indicated antibodies as described above.

### 2.10. Ubiquitylation assay

293T cells were transfected with 2 μg total of the indicated plasmids using JetPRIME reagent (PolyPLUS) according to the manufacturer's guidelines. Forty-eight hours after

transfection, cells were stimulated with 100 ng/mL PMA for 1 hour, the PMA was washed out, and the cells were lysed 5 hours later with a solution containing 50 mM Tris-HCl, pH 7.4, 150 mM NaCl, 0.5% Triton X-100, 5 mM EDTA, 2 mM sodium orthovanadate, 10 mM iodoacetamide, and protease cocktail inhibitors (Thermo Scientific). After reserving 3% of the cell lysate to run as input, the remainder was pre-cleared with protein A/G agarose beads (Santa Cruz Biotechnology) and then incubated with 1 μg of anti-Cx43 (71–0700, Invitrogen) antibody, 2 μg of anti-HA (H9658, Sigma) antibody, or control anti-rabbit IgG overnight as indicated. The next day, the immunocomplexes were incubated with protein A/G agarose beads (Santa Cruz Biotechnology) for three hours, washed in lysis buffer, eluted with 2X Laemmli sample buffer after boiling for 5 min at 95°C, resolved using SDS-PAGE, and blotted with the indicated antibodies.

### 2.11. Statistics

Statistical analysis of quantitative data (mean, standard deviation, 2-tailed unpaired t-test for comparison of means, and one-factor analysis of variance corrected by the post hoc Tukey test for multiple comparisons) and Kaplan-Meier survival analysis were calculated and plotted using Prism software (GraphPad Software Inc). All cell culture experiments were performed at least three independent times with similar results. Numbers of animals used per experiment is indicated in the appropriate figure legends.

## 3. Results

### 3.1. Inducible overexpression of Wwp1 in an animal model

Because increases in the expression of WWP1 have been associated with carcinogenesis and with aging [21], a novel inducible transgenic system called pTraffic was created to model these pathologies *in vivo*. In this system, the presence of the inactive (*i.e.*, not expressing) *Wwp1* transgene is marked by ubiquitous DsRed2 fluorescence (Fig. 1A). The transgene can be activated in a tissue- and temporal-specific manner upon exposure to the cre recombinase, which mediates recombination between the two loxP sites in the vector (Fig. 1B). This results in the loss of DsRed2 fluorescence, the increased expression of Wwp1, and the gain of eGFP fluorescence, which is expressed from an internal ribosome entry sequence. Thus, all cells that have undergone cre-mediated recombination will fluoresce green instead of red.

This construct was injected into fertilized pronuclei to create transgenic founders. As expected, the founders ubiquitously expressed the DsRed2 tag in the skin whereas no eGFP could be visualized (Fig. 1A). We selected those founders (numbers 14667 and 14730) that displayed the highest expression of DsRed2 with the lowest vector copy number to minimize the possibility of obtaining strange recombination products from concatamers of unknown orientation in order to create two independent lines (data not shown). To determine whether Wwp1 can regulate Cx43 in a number of tissues, the overexpression of Wwp1 was activated ubiquitously by breeding the pTraffic lines to homozygous β-actin cre animals to yield offspring with just the cre construct (+/+; cre/+, also referred to as wild type or WT) as well as littermates with the activated pTraffic and cre transgenes (tg/+; cre/+).

### 3.2. Mice that globally overexpress Wwp1 develop LVH and die around 8 weeks of age

Whereas mice carrying the inactive pTraffic transgene were found to have a normal life span, mice globally overexpressing Wwp1 died suddenly without any previous signs of illness between five and thirteen weeks of age, and this phenotype was completely penetrant in both independent founder lines (Fig. 1C). The median age of survival in the 14667 line was 62.5 days and 55.5 days in the 14730 line, both statistically significantly different from the WT (+/+; cre/+) littermates but not from one another. The only change noted on gross necropsy and histopathologic evaluation of major organ systems of Wwp1 overexpressers from both lines was an overall globular shape to the heart with mild to moderate LVH but no dilation in any of the four chambers as compared to cre-only WT littermate controls (data not shown). There was also a statistically significant increase in heart weight-to-body weight and heart weight-to-tibia length ratios in both lines (Supplementary Table 1).

While the gross necropsy suggested that the phenotype might arise as a consequence of cardiac abnormalities, since the cre transgene is ubiquitously expressed in these animals, it was likely that Wwp1 was activated to differing degrees in various tissues throughout the body. To quantify the degree of Wwp1 upregulation, the expression of *Wwp1* was evaluated in a number of tissues derived from two tg/+; cre/+ males and two tg/+; cre/+ females from each line in comparison to two gender- and age-matched +/+; cre/+ littermates from each line using quantitative real time PCR. Representative results of detected fold increase in *Wwp1* mRNA in brain, heart, bone marrow-derived leukocytes ($CD45^+$), kidney, liver, lungs, bone marrow-derived mesenchymal stem cells ($CD45^-$), spleen, and thymus are shown in Fig. 1D. While a statistically significant increase in the fold-change of *Wwp1* (ranging from 1.8- to 4-fold) was detected in all tissues except bone marrow-derived mesenchymal stem-like cells, the highest increase in *Wwp1* mRNA expression was detected in the heart (~24-fold increase), consistent with the altered gross histology of these animals (Fig. 1D).

The LVH noted on gross histology was corroborated by examining the expression of hypertrophic markers using quantitative real time PCR. Consistent with LVH and a reactivation of fetal growth genes, *Nppb*, *Nppa*, and *Myh7* were all significantly upregulated in hearts of the Wwp1 overexpressers relative to WT cre-only littermate controls (Fig. 2A). Additionally, quantification of cardiomyocyte fiber cross sectional surface area highlighted by WGA staining of the sarcolemma revealed a significant increase in each transgenic line, in keeping with presumptive concentric hypertrophy in these animals (Fig. 2B). Cardiac structure and function were more precisely analyzed in Wwp1 overexpressers using longitudinal echocardiographic studies. By eight weeks of age, Wwp1 overexpressers from both the 14667 and 14730 lines displayed statistically significant LVH (particularly in the posterior wall) without any evidence of compromised ventricular function (Fig. 2C and Supplementary Table 1, n=6 for each genotype). Rather, there was a slight but statistically significant increase in both ejection fraction and fractional shortening in both lines (Supplementary Table 1). Thus, the detected LVH was not responsible for overt heart failure. However, arrhythmic traces and irregular heartbeats were observed in the majority of the Wwp1 overexpressers from both lines between six and eight weeks of age whereas none of the cre-only littermates displayed such abnormalities (Fig. 2C).

### 3.3. Animals overexpressing Wwp1 have ventricular arrhythmias

To further characterize the apparent arrhythmias observed in Wwp1 overexpressers during echocardiography, electrocardiographic analysis was performed on these animals. Analysis of eight Wwp1 transgenic animals and their WT (+/+; cre/+) littermates from each line revealed that Wwp1 overexpressers possessed decreased amplitude of waveforms along with a significant widening of the QRS complex and a prolonged QT corrected interval in both the 14667 and 14730 lines (Supplementary Table 2). These results are consistent with defects in ventricular conduction and repolarization, which has also been noted in animals lacking Cx43 [33] and suggests that the cause of sudden death might be related to ventricular arrhythmias.

This hypothesis was confirmed by isolating hearts from Wwp1 overexpressors (n=9) and from their WT cre-only littermates (n=7) and subjecting them to an overdrive pacing protocol while recording the electrocardiograms. Shown in Fig. 3A are typical electrocardiogram traces from these hearts before and after 1.5 sec rapid pacing. The abnormal baseline waveforms noted for the Wwp1 overexpressers were similar to those observed *in vivo* in the whole animal. During these experiments, all wild type hearts quickly recovered sinus rhythm while all the hearts derived from Wwp1 overexpressers displayed ventricular arrhythmias. In fact, in two of the nine hearts derived from Wwp1 overexpressers, spontaneous sustained tachycardia was observed (Fig. 3B) which was assumed to be lethal *in vivo*. In total, all nine hearts derived from Wwp1 overexpressing animals displayed multiple arrhythmias, and seven of the nine hearts demonstrated sustained tachycardia (either spontaneous or pacing-induced) that is likely lethal in the animal. In contrast, five of the seven hearts derived from wild type animals showed no detectable arrhythmia after multiple installments of overdrive pacing, while the remaining two displayed only one arrhythmic episode followed by rapid recovery of sinus rhythm over the course of the entire experiment (Fig. 3C), thus suggesting that the cause of sudden death in Wwp1 overexpressing animals is lethal ventricular arrhythmias.

### 3.4. Hearts derived from animals overexpressing Wwp1 display GJ remodeling and almost a complete loss of Cx43 protein

To ascertain whether Wwp1 overexpressers displayed GJ remodeling, cryostat sections from Wwp1 overexpressers (n=4) from the 14667 and the 14730 lines as well as from WT cre-only littermates (n=4) were co-immunostained for phalloidin, Cx43, and either N-cadherin or desmoplakin. While Cx43 almost completely localized to the intercalated discs of 8 week old WT (+/+; cre/+) mice, there were greatly reduced amounts and generalized mislocalization of Cx43 in Wwp1 overexpressers (tg/+; cre/+) at that age (Fig. 4A). The effect of Wwp1 overexpression appeared to be specific to Cx43 and not symptomatic of global structural alterations affecting the intercalated disc as no change in N-cadherin or desmoplakin expression was noted (Fig. 4A and 4B). This staining pattern is consistent with either increased internalization and/or increased degradation of GJs. To distinguish between these possibilities, total protein extracts were prepared from hearts of Wwp1 overexpressers and WT littermates and Cx43 levels were analyzed by Western blotting (Fig. 4B). Quantification of Cx43 levels indicated that overexpression of Wwp1 resulted in a statistically significant reduction of Cx43 protein levels in both lines (88% in 14667 and

87% in 14730; Fig. 4C). In contrast, no change in the protein levels of Cx40 or Cx45, the two other connexins highly expressed in the heart, were observed (Supplementary Fig. 1), again corroborating the specificity of the effect of Wwp1 on Cx43. Interestingly, the observed Wwp1-induced changes in Cx43 localization and expression were solely at the protein level as quantitative real time PCR detected no significant change in *Cx43* mRNA levels in either Wwp1 overexpressing line relative to the WT littermates (Fig. 4D), suggesting that the direct or indirect regulation of Cx43 by Wwp1 was post-translational.

### 3.5. Wwp1 interacts with and ubiquitylates Cx43

Since Wwp1 is an E3 ubiquitin ligase, we hypothesized that it might bind to and ubiquitylate Cx43, causing its degradation during GJ turnover or pathological GJ remodeling. To first determine whether endogenous Wwp1 and Cx43 co-localized in the heart, we performed co-immunofluorescent labeling of paraffin sections of normal human heart (n=3) since, in our hands, the anti-Wwp1 antibody would not recognize endogenous mouse Wwp1. The results of this experiment showed colocalization of WWP1 and Cx43 intracellularly within small discrete puncta of cardiomyocytes (Supplementary Fig. 2), suggesting that Wwp1 might act on internalized Cx43 to promote its degradation. Because co-localization of Wwp1 and Cx43 was limited to small intracellular subsets of these proteins and because the interaction between an ubiquitin ligase and a putative substrate is transitory in nature, co-immunoprecipitation of exogenously expressed Cx43 and Wwp1 was performed in 293T cells to maximize the probability of success. In particular, 293T cells were transiently transfected with Cx43 and either mCherry/MYC tandem tagged WT Wwp1 or a mCherry/MYC tandem-tagged mutant Wwp1 in which the E3 activity has been abolished by a point mutation (herein referred to as MYC-C886S, both constructs were previously described in [34]). Forty-eight hours after transfection, cells were stimulated with PMA to promote the internalization and ubiquitylation of Cx43 [35]. We found that similar amounts of WT and mutant Wwp1 co-immunoprecipitated with Cx43 and that this interaction was independent of the ubiquitin ligase activity of Wwp1 (Fig. 5A, lanes 1 and 2). However, co-immunoprecipitation of Cx43 and Wwp1 was dependent upon an intact PY motif in Cx43 as the P283L mutant (in which the first proline of the PPXY module of Cx43 had been mutated to leucine) was unable to pull down Wwp1 *in vivo* (Fig. 5A, lanes 7 and 8), suggesting that this motif may interact with the WW domains of Wwp1 as has previously been described for the Nedd4-Cx43 association [16]. This effect was likely not caused by a dominant negative effect of the P283L mutant as our 293T cells do not express appreciable amounts of Cx43 (Fig. 5A, input lanes 4–6). Importantly, the observed interaction between Cx43 and Wwp1 was specific in that no Wwp1 was detected in either samples that were immunoprecipitated with a rabbit IgG negative control (Fig. 5A, right panels) or in cells transfected with empty vector subjected to Cx43 immunoprecipitation (Fig. 5A, left panels, lane 6).

Interestingly, we observed that when WT Wwp1 was co-expressed with Cx43, there was less steady state Cx43 detected in the input, but this effect was abrogated by expressing the ligase-dead version of Wwp1 (Fig 5A, Cx43 input lanes 1 vs. 2), suggesting that Wwp1 might promote the ubiquitylation and subsequent degradation of Cx43. This hypothesis was tested by transiently transfecting 293T cells with hemagglutinin (HA)-tagged Ub (previously described in [36]), Cx43, and either MYC-Wwp1 or MYC-C886S. Forty-eight hours after

transfection, cells were stimulated with 100 ng/mL PMA for 60 min, and, after wash out, cells were incubated in complete media for another 5 hours as this was determined to maximize the detectable ubiquitylation of Cx43 (Supplementary Figure 3). Ubiquitylation of Cx43 was assessed by immunoprecipitating the indicated cellular lysates with anti-Cx43 antibody and then immunoblotting with anti-HA. This assay revealed that Wwp1 could mediate robust ubiquitylation of Cx43 (lane 1, Fig. 5B), and that this modification of Cx43 was dependent upon the intact Ub ligase activity of Wwp1, as catalytically inactive Wwp1 (MYC-C886S, lane 2, Fig. 5B) showed markedly reduced ubiquitylation of Cx43 with an apparent increase in the steady state levels of Cx43 comparable to exogenous expression of Cx43 alone (Cx43 input, lane 1 vs. lanes 2 and 4, Fig. 5B). No ubiquitylation of Cx43 was detected with just Cx43 or just HA-Ub (lanes 3 and 4, Fig. 5B) or when lysates were subjected to immunoprecipitation with a rabbit IgG negative control (Fig. 5B, right panels). Ubiquitylation of Cx43 rather than another Cx43-interacting protein that might precipitate in the immunocomplex was confirmed by performing a reverse ubiquitylation assay in which lysates from 293T cells transiently transfected with the indicated plasmids and PMA stimulated 293T cells were immunoprecipiated with anti-HA antibody and then immunoblotted with anti-Cx43. Once again, laddering of high molecular weight proteins was observed in cells transfected with WT Wwp1 whereas these additional bands were not seen when MYC-C886 was expressed (Supplemental Fig. 4), consistent with the assertion that overexpression of Wwp1 promotes the ubiquitylation of Cx43. Given the dramatic decrease in Cx43 protein in the hearts of Wwp1 overexpressers, it is tempting to speculate that this ubiquitylation event might promote the degradation of Cx43, predisposing them to ventricular arrhythmias.

### 3.6. Cardiomyocyte-specific overexpression of Wwp1 phenocopies global Wwp1 induction

Although global Wwp1 overexpressers displayed ventricular arrhythmias, the sudden cardiac death phenotype might have arisen as a secondary, downstream consequence of the myocardial, structural remodeling and LVH rather than as a result of the direct effects on Cx43. To tease apart this mechanism, we crossed the pTraffic-Wwp1 transgenics to mice homozygous for a tamoxifen (Tmx)-inducible cre under the control of the cardiomyocyte-specific alpha -myosin heavy chain promoter (MerCreMer) [37], yielding offspring that carried just the cre construct (+/+; MerCreMer/+) or animals that carried both the pTraffic-Wwp1 and MerCreMer transgenes (tg/+; MerCreMer/+). Mice bearing the MerCreMer transgene do not robustly express cre until exposed to a sufficient dosage of Tmx, as the cre is under the control of mutant estrogen receptors; however, a low level of leakiness due to responsiveness to endogenous estrogens has been noted in these animals [37]. To dissect the temporal contribution of Wwp1 overexpression to the sudden cardiac death phenotype, we intraperitoneally injected cohorts of at least 10 mice on two consecutive days with either 40 mg/kg of vehicle or with 40 mg/kg of Tmx beginning either at 26 days of age or at 54 days of age. All cre only mice (+/+; MerCreMer/+) receiving either vehicle or Tmx injections as well as Wwp1 transgenic mice (tg/+; MerCreMer/+) receiving vehicle injections had a normal lifespan while Tmx-injected tg/+; MerCreMer/+ mice survived to about 8 weeks of age (Fig. 6A), similar to what was seen in the global overexpressers. In particular, the median age of survival of tg/+; MerCreMer/+ injected with Tmx at 26 days of age was 55 days, whereas the median age of survival for cardiomyocyte-specific overexpression

initiated at 54 days of age was 57 days, three days after the first injection of Tmx. Interestingly, when these mice were examined using echocardiography, LVH was only noted in those tg/+; MerCreMer/+ mice that had been Tmx-treated beginning at 26 days of age and this hypertrophy took at least 18 days to appear (Fig. 6B). In contrast, none of the tg/+; MerCreMer/+ mice receiving Tmx injections beginning at 54 days of age survived beyond 59 days of age (*i.e*., five days following the first injection), and no LVH was detected by echocardiography. However, as early as one day following the first injection, an irregular heartbeat was detected in some of this cohort (Fig. 6B).

Because maximal induction of the transgene by Tmx was reached 72 hours following the first injection (Supplementary Fig. 5), that time point was utilized to evaluate the levels of Cx43 in tg/+; MerCreMer/+ animals injected with either vehicle or with Tmx at 26 and at 54 days of age. Irrespective of when Tmx was administered, it caused an activation of the pTraffic-Wwp1 transgene and a resulting ~40% decrease (38% decrease when Tmx was administered at 26 days or 45% decrease when Tmx was injected at 54 days of age) in Cx43 protein detected in total heart protein extracts by Western blot as compared to vehicle-injected tg/+; MerCreMer/+ or to treated cre-only controls (Fig. 7A). Since myocytes have been reported to make up 55% of the mouse heart [38], this decrease in Cx43 would translate to a 69–82% decrease in Cx43 within cardiomyocytes. Indeed, when cryostat sections of hearts derived from Tmx- or vehicle-treated tg/+; MerCreMer/+ were immunostained for phalloidin and Cx43, we could detect very little Cx43 in the myocytes of tg/+; MerCreMer/+ animals that had been Tmx-treated either at 26 or at 54 days of age (Supplementary Fig. 6). Thus, this aspect of cardiomyocyte-specific overexpression of Wwp1 was very similar to what was observed with global overexpression of Wwp1.

Reduction in myocardial Cx43 would be expected to influence electroconduction of the heart. To assess this possibility in tg/+; MerCreMer/+ mice, electrocardiogram studies were conducted. In particular, since cardiomyocyte-specific overexpression of Wwp1 at 26 days of age resulted in markedly decreased Cx43 within 72 hours but death was not evidenced until 55 days of age, we hypothesized that lack of GJ intercellular communication in the myocardium would be sufficient to create an arrhythmogenic substrate that would be revealed when stressed. This hypothesis was tested by injecting three tg/+; MerCreMer/+ mice with vehicle and another three mice with Tmx at 26 days of age. One week later (before LVH was detectable, Fig. 6B), hearts were isolated from these animals and subjected to an overdrive pacing protocol while electrocardiographic measurements were taken. Baseline readings on Langendorff-perfused hearts obtained from Tmx-treated tg/+; MerCreMer/+ animals showed electroconduction abnormalities including a reduced QRS amplitude and a prolonged QT interval, whereas none were noted in hearts derived from tg/+; MerCreMer/+ that had received vehicle injections the week before (Fig. 7B). When subjected to 1.5 second rapid cardiac pacing, the hearts from vehicle-injected double transgenic mice quickly recovered normal sinus rhythm. However, hearts derived from the Tmx-treated double transgenic animals subjected to the same pacing protocol exhibited ventricular fibrillation that *in vivo* would likely result in sudden cardiac death (Fig. 7B). Taken together, these results indicate that cardiomyocyte-specific overexpression of Wwp1 beginning at approximately 4 weeks of age makes the heart highly susceptible to

arrhythmogenesis, yet pathways exist to compensate for the lack of Cx43 during this phase of postnatal development allowing the animals to survive to early adulthood.

Because mice overexpressing Wwp1 either globally or in just the cardiomyocytes lived to approximately 8 weeks of age, it stands to reason that activation of the Wwp1 transgene in tg/+; MerCreMer/+ animals at 54 days of age would yield a rapid deterioration of the ventricular electroconduction signal that correlated with the loss of Cx43 and onset of sudden cardiac death. This assertion was tested by serially recording surface electrocardiograms from four 54 day old mice injected with vehicle and from another four 54 day old mice injected with Tmx. Baseline electrocardiograms were obtained before injection and then again at 12, 24, 48, and 72 hours following injection in the same cohort of animals (Fig. 7C). These experiments revealed a significant decrease in the amplitude of the QRS interval at both the 12 and 24 hour time points in Tmx-treated animals, indicative of decreased electroconduction in the ventricles associated with the initial activation of Wwp1. At the 48 and 72 hour time points, Tmx-treated animals showed further reduction in the QRS amplitude as well as prolongation of the QT interval, a precursor to arrhythogenesis, with almost undetectable waveforms in some of the animals at 72 hours (Fig. 7C). None of the Tmx-injected animals survived beyond 72 hours, expiring from what was likely ventricular arrhythmogenic episodes in the absence of any LVH (Fig. 6C). In contrast, all vehicle-injected animals displayed no significant changes in their EKG traces compared to their baseline recordings over the time period examined (Fig. 7C).

## 4. Discussion

The studies presented here reveal the critical and previously unappreciated cell autonomous role of Wwp1 in modulating Cx43 stability in the myocardium via its ability to bind to and ubiquitylate Cx43. Global- and cardiomyocyte-specific overexpression of Wwp1 both resulted in the generation of lethal ventricular arrhythmias around 8 weeks of age due to the dramatic reduction of Cx43 protein in the heart muscle. In humans, heterozygous (and a few homozygous) germline mutations in *GJA1* cause ODDD with congenital craniofacial abnormalities, soft tissue fusion of the digits, small eyes, and anomalies of the teeth including loss of enamel (reviewed in [39]). Further, these phenotypes can also present as part of a syndrome that includes neuropathies, skin disease, bladder incontinence, thermosensitivity, lymphedema, and, rarely, arrhythmia [29]. In mouse, constitutive knockout of *Gja1* yielded a phenotype of perinatal mortality due to malformations in the right ventricular outflow tract,[40] whereas cardiomyocyte-specific inactivation of *Gja1* resulted in lethal ventricular arrhythmias without any structural alterations by two months of age despite a 86–95% decrease in Cx43 protein detected as early as E12.5 [41]. This phenotype is identical to what we observed upon cardiomyocyte-specific activation of Wwp1 at 54 days of age and very similar to our global overexpressers. The particularly high level of *Wwp1* overexpression induced in the heart relative to brain (a representative neural tissue) or bone marrow-derived $CD45^{-}$ mesenchymal stem-like cells likely accounts for the lack of bone or neurological phenotypes in our global overexpressers, despite the prominent role played by both Cx43 and Wwp1 in these other tissues.

It is interesting to note that, so long as no trigger is applied, the timing of the spontaneous sudden cardiac death at ~8 weeks of age was very consistent in Wwp1 overexpressing animals, irrespective of whether the overexpression was global or cardiomyocyte-specific (initiated at either 26 days or 54 days of age) and regardless of whether LVH is present. The onset of spontaneous sudden cardiac death did not appear to depend on the kinetics of Cx43 loss, as a similar decrease in Cx43 protein in the cardiomyocytes of Tmx-treated tg/+; MerCreMer/+ animals was noted within 72h of injection at both 26 and at 54 days of age relative to vehicle-injected tg/+; MerCreMer/+ littermates (Fig. 7A). It remains a formal possibility that this small difference in Cx43 expression between four and eight weeks of age, while not statistically significant, may be physiologically relevant in producing enough of a buffer against spontaneous reentry arrhythmia similar to what has been described in the O-CKO line of Cx43 cardiomyocyte-specific loss of function animals [33]. However, this decrease in Cx43 associated with early activation of Wwp1 is sufficient to render the animals susceptible to induced arrhythmias at this age (Fig. 7B). Spontaneous sudden cardiac death manifesting around two months of age in our Wwp1 overexpressers as well as in cardiomyocyte-specific knockout of Cx43 [41] may reflect developmental programs in the murine heart. Eight weeks of age corresponds to the point of postnatal cardiac development in mouse where the architecture of the cardiomyocytes has reached its full maturity and where Cx43 localizes exclusively to the intercalated discs [42]. As such, it would appear that the still developing postnatal heart is a dynamic entity with much more plasticity of gene expression, allowing it to cope with alterations in electroconduction that accompany a 69–82% decrease of Cx43 protein in the myocardium arising from either conditional loss of Cx43 or from overexpression of Wwp1.

Wwp1 belongs to the same subfamily of HECT E3s as Nedd4 and Smurf2, ubiquitin ligases that have previously been shown to contribute to the downregulation of Cx43 in cell culture systems either directly or indirectly [14–16]. All members of this subfamily are widely expressed with numerous other substrates and alternative splice isoforms reported for many of them [17], prompting the questions of whether these ligases serve redundant roles in targeting Cx43 and/or associated proteins, or, if not, how is specificity in various cellular, tissue, and biological contexts achieved? Interestingly, *Nedd4* knockout mice die *in utero* around mid-gestation with marked heart defects including double-outlet right ventricle and atrioventricular cushion defects as well as vascular anomalies [43], indicating that Nedd4 plays an essential role early on in heart development and may act on cardiac-specific targets other than Cx43. Further, a recent report found a correlation between the downregulation of *SMURF2* mRNA and the pathogenesis of dilated cardiomyopathy as opposed to ischemic cardiomyopathy in a cohort of 31 patients[44] which would suggest that this ligase may be more important in the homeostasis of adult cardiomyocytes. Certainly the work described here illustrates that the longest isoform of Wwp1 (which has been the best characterized in the literature) plays an important role in the cellular homeostasis and rapid turnover of Cx43 *in vivo*, as mice expressing increased Wwp1 in the heart universally developed lethal ventricular arrhythmias as a consequence of the pathological GJ remodeling. Importantly, this phenotype was completely penetrant in two independent founder lines and was robust to differences in strain background, as the β-actin cre line used to create the global overepressers was on a FVB/N background whereas the MerCreMer animals were on a

mixed B6/129 background. Strain background effects have been reported to modulate conduction disease severity in mice with cardiac sodium channelopathies, with the 129P2 background contributing to greater severity of the phenotype than FVB/N [45, 46]. The phenotype described here is unlikely to be an overexpression artifact, as we have observed that *Wwp1*$^{-/-}$ animals have increased amounts of cardiac Cx43 protein and longer GJs at the intercalated discs, consistent with a physiological role for Wwp1 in Cx43 homeostasis (W. A. Basheer, R. L. Price, and L. E. Matesic, manuscript in preparation).

In addition to arrhythmogenesis, mild-to-moderate LVH with concentric hypertrophy of cardiomyocytes was noted in mice overexpressing Wwp1 either globally or exclusively in the cardiomyocytes beginning at 26 days of age. Because LVH has not been associated with cardiomyocyte-specific loss of Cx43 function [41], it may be that the cellular overgrowth observed in our overexpressers results from Cx43-independent pathways. Among its many known targets, Wwp1 has been shown to regulate the tumor suppressor LATS1 in breast cancer cells and target it for proteasomal degradation [47]. LATS1/2 are negative regulators of Hippo signaling, an evolutionarily conserved pathway involved in development, stem cell function, regeneration, and regulation of organ size in various tissues including the heart (reviewed in [48]). In particular, activation of Hippo signaling via the conditional overexpression of wild-type Yap in neonatal cardiomyocytes was noted to increase the size of the cells and to induce the expression of *Nppa*, *Nppb*, and the β-myosin heavy chain [49]. Further, using both gain of function and loss of function approaches, it has been shown that Lats2, a paralog of Lats1 highly expressed in the mammalian heart, is a negative regulator of cardiomyocyte size both in the postnatal period as well as in adult animals in response to pathological stress like pressure overload [50]. Thus, it is tempting to speculate that overexpression of Wwp1 in the early postnatal period increases Hippo signaling and promotes hypertrophy of cardiomyocytes, contributing to the LVH phenotype observed in our animals.

While the physiological role of Wwp1 in whole animals still needs to be examined more thoroughly, the studies described here offer novel insights into GJ turnover and remodeling. In particular, they define an association between the upregulation of Wwp1 in the heart and the downregulation of Cx43 leading to lethal ventricular arrhythmias in mice. Mechanistically, this likely arises from the ubiquitylation of Cx43, prompting its internalization from the intercalated disc and/or degradation. Research currently underway suggests that Wwp1 may be important in regulating the recycling of Cx43 (M. Abreha, H. L. Mentrup, and L. E. Matesic, manuscript in preparation). Thus, it may be that in animals overexpressing Wwp1, the decrease in steady state Cx43 protein results from increased degradation and decreased recycling without any change in the normal internalization of the protein. It would be predicted that increased Wwp1 expression would have an even more drastic outcome when internalization of Cx43 is promoted via phosphorylation during ischemia [51] or with PMA treatment [35]. Although there are outstanding questions regarding how the expression of *Wwp1* is controlled and its potential role in regulating other targets, it will be interesting to determine whether WWP1 is similarly increased in acquired and genetic models of arrhythmogenesis in humans. Identification of this new molecular player involved in the regulation of Cx43 provides inroads towards a prospective new class

of therapeutic targets for the treatment of ventricular arrhythmias and sudden cardiac death, as WWP1 and other HECT E3s have recently been described to be druggable by peptide and small molecule inhibitors [52]. Since the incidence of sudden cardiac death is estimated to be in the range of 50–100 per 100,000 persons in industrialized nations per annum [53], this possibility certainly necessitates further consideration.

## Supplementary Material

Refer to Web version on PubMed Central for supplementary material.

## Acknowledgements

The authors gratefully acknowledge Dr. Robert Gourdie and Jane Jourdan (Virginia Tech Carilion Research Institute, Roanoke, VA) for helpful advice regarding Cx43 tissue Westerns. We thank Dr. Ceshi Chen (Kunming Institute of Zoology, Chinese Academy of Sciences) for providing the MYC-Wwp1 and MYC-Wwp1 C886 expression constructs, Dr. Alan Lau (University of Hawaii Cancer Center, Honolulu, HI) for providing the Cx43 expression plasmid, and Dr. Adam Dupuy (University of Iowa School of Medicine, Iowa City, IA) for providing the pRedInC plasmid.

**Sources of Funding**

This work was supported by the National Institutes of Health [R01HL104030 to L.E.M.], the American Heart Association [10SDG2650005 to L.E.M.], and the intramural research program of the National Institutes of Health, National Cancer Institute, Center for Cancer Research [N.G.C. and N.A.J.].

## Abbreviations

| | |
|---|---|
| **Cx43** | connexin 43 |
| **E1** | ubiquitin activating enzyme |
| **E2** | ubiquitin conjugating enzyme |
| **E3** | ubiquitin ligase |
| **GJ** | gap junctions |
| **HA** | hemagglutinin |
| **HECT** | homologous to E6-AP carboxy terminus |
| **LVH** | left ventricular hypertrophy |
| **ODDD** | oculodentodigital dysplasia |
| **PMA** | phorbol 12-myristate 13-acetate |
| **RING** | really interesting new gene |
| **Tmx** | tamoxifen |
| **Ub** | ubiquitin |
| **WGA** | wheat germ agglutinin |
| **WT** | wild type |

## References


1. Jones SA, Lancaster MK, Boyett MR. Ageing-related changes of connexins and conduction within the sinoatrial node. J Physiol. 2004; 560:429–437. [PubMed: 15308686]
2. Severs NJ, Bruce AF, Dupont E, Rothery S. Remodelling of gap junctions and connexin expression in diseased myocardium. Cardiovascular research. 2008; 80:9–19. [PubMed: 18519446]
3. Remo BF, Giovannone S, Fishman GI. Connexin43 cardiac gap junction remodeling: lessons from genetically engineered murine models. The Journal of membrane biology. 2012; 245:275–281. [PubMed: 22722763]
4. Beardslee MA, Laing JG, Beyer EC, Saffitz JE. Rapid turnover of connexin43 in the adult rat heart. Circulation research. 1998; 83:629–635. [PubMed: 9742058]
5. Darrow BJ, Laing JG, Lampe PD, Saffitz JE, Beyer EC. Expression of multiple connexins in cultured neonatal rat ventricular myocytes. Circulation research. 1995; 76:381–387. [PubMed: 7859384]
6. Laird DW, Puranam KL, Revel JP. Turnover and phosphorylation dynamics of connexin43 gap junction protein in cultured cardiac myocytes. The Biochemical journal. 1991; 273(Pt 1):67–72. [PubMed: 1846532]
7. Kjenseth A, Fykerud T, Rivedal E, Leithe E. Regulation of gap junction intercellular communication by the ubiquitin system. Cell Signal. 2010; 22:1267–1273. [PubMed: 20206687]
8. Su V, Lau AF. Ubiquitination, intracellular trafficking, and degradation of connexins. Arch Biochem Biophys. 2012; 524:16–22. [PubMed: 22239989]
9. Martins-Marques T, Catarino S, Marques C, Matafome P, Ribeiro-Rodrigues T, Baptista R, et al. Heart ischemia results in connexin43 ubiquitination localized at the intercalated discs. Biochimie. 2015; 112:196–201. [PubMed: 25748165]
10. Martins-Marques T, Catarino S, Zuzarte M, Marques C, Matafome P, Pereira P, et al. Ischaemia-induced autophagy leads to degradation of gap junction protein connexin43 in cardiomyocytes. The Biochemical journal. 2015; 467:231–245. [PubMed: 25605500]
11. Popovic D, Vucic D, Dikic I. Ubiquitination in disease pathogenesis and treatment. Nature medicine. 2014; 20:1242–1253.
12. Hicke L, Dunn R. Regulation of membrane protein transport by ubiquitin and ubiquitin-binding proteins. Annual review of cell and developmental biology. 2003; 19:141–172.
13. Chen VC, Kristensen AR, Foster LJ, Naus CC. Association of connexin43 with E3 ubiquitin ligase TRIM21 reveals a mechanism for gap junction phosphodegron control. J Proteome Res. 2012; 11:6134–6146. [PubMed: 23106098]
14. Fykerud TA, Kjenseth A, Schink KO, Sirnes S, Bruun J, Omori Y, et al. Smad ubiquitination regulatory factor-2 controls gap junction intercellular communication by modulating endocytosis and degradation of connexin43. Journal of cell science. 2012; 125:3966–3976. [PubMed: 22623726]
15. Girao H, Catarino S, Pereira P. Eps15 interacts with ubiquitinated Cx43 and mediates its internalization. Exp Cell Res. 2009; 315:3587–3597. [PubMed: 19835873]
16. Leykauf K, Salek M, Bomke J, Frech M, Lehmann WD, Durst M, et al. Ubiquitin protein ligase Nedd4 binds to connexin43 by a phosphorylation-modulated process. Journal of cell science. 2006; 119:3634–3642. [PubMed: 16931598]
17. Chen C, Matesic LE. The Nedd4-like family of E3 ubiquitin ligases and cancer. Cancer metastasis reviews. 2007; 26:587–604. [PubMed: 17726579]
18. Komuro A, Imamura T, Saitoh M, Yoshida Y, Yamori T, Miyazono K, et al. Negative regulation of transforming growth factor-beta (TGF-beta) signaling by WW domain-containing protein 1 (WWP1). Oncogene. 2004; 23:6914–6923. [PubMed: 15221015]
19. Mosser EA, Kasanov JD, Forsberg EC, Kay BK, Ney PA, Bresnick EH. Physical and functional interactions between the transactivation domain of the hematopoietic transcription factor NF-E2 and WW domains. Biochemistry. 1998; 37:13686–13695. [PubMed: 9753456]
20. Wood JD, Yuan J, Margolis RL, Colomer V, Duan K, Kushi J, et al. Atrophin-1, the DRPLA gene product, interacts with two families of WW domain-containing proteins. Mol Cell Neurosci. 1998; 11:149–160. [PubMed: 9647693]

21. Zhi X, Chen C. WWP1: a versatile ubiquitin E3 ligase in signaling and diseases. Cell Mol Life Sci. 2012; 69:1425–1434. [PubMed: 22051607]
22. Chen C, Sun X, Guo P, Dong XY, Sethi P, Zhou W, et al. Ubiquitin E3 ligase WWP1 as an oncogenic factor in human prostate cancer. Oncogene. 2007; 26:2386–2394. [PubMed: 17016436]
23. Chen C, Zhou Z, Ross JS, Zhou W, Dong JT. The amplified WWP1 gene is a potential molecular target in breast cancer. Int J Cancer. 2007; 121:80–87. [PubMed: 17330240]
24. Cheng Q, Cao X, Yuan F, Li G, Tong T. Knockdown of WWP1 inhibits growth and induces apoptosis in hepatoma carcinoma cells through the activation of caspase3 and p53. Biochemical and biophysical research communications. 2014; 448:248–254. [PubMed: 24792179]
25. Lin JH, Hsieh SC, Chen JN, Tsai MH, Chang CC. WWP1 gene is a potential molecular target of human oral cancer. Oral Surg Oral Med Oral Pathol Oral Radiol. 2013; 116:221–231. [PubMed: 23849376]
26. Zhang L, Wu Z, Ma Z, Liu H, Wu Y, Zhang Q. WWP1 as a potential tumor oncogene regulates PTEN-Akt signaling pathway in human gastric carcinoma. Tumour Biol. 2015; 36:787–798. [PubMed: 25293520]
27. Shu L, Zhang H, Boyce BF, Xing L. Ubiquitin E3 ligase Wwp1 negatively regulates osteoblast function by inhibiting osteoblast differentiation and migration. J Bone Miner Res. 2013; 28:1925–1935. [PubMed: 23553732]
28. Batra N, Kar R, Jiang JX. Gap junctions and hemichannels in signal transmission, function and development of bone. Biochimica et biophysica acta. 2012; 1818:1909–1918. [PubMed: 21963408]
29. Paznekas WA, Karczeski B, Vermeer S, Lowry RB, Delatycki M, Laurence F, et al. GJA1 mutations, variants, and connexin 43 dysfunction as it relates to the oculodentodigital dysplasia phenotype. Hum Mutat. 2009; 30:724–733. [PubMed: 19338053]
30. Naus CC, Laird DW. Implications and challenges of connexin connections to cancer. Nat Rev Cancer. 2010; 10:435–441. [PubMed: 20495577]
31. Andersson KB, Winer LH, Mork HK, Molkentin JD, Jaisser F. Tamoxifen administration routes and dosage for inducible Cre-mediated gene disruption in mouse hearts. Transgenic Res. 2010; 19:715–725. [PubMed: 19894134]
32. Pfaffl MW, Georgieva TM, Georgiev IP, Ontsouka E, Hageleit M, Blum JW. Real-time RT-PCR quantification of insulin-like growth factor (IGF)-1, IGF-1 receptor, IGF-2, IGF-2 receptor, insulin receptor, growth hormone receptor, IGF-binding proteins 1, 2 and 3 in the bovine species. Domest Anim Endocrinol. 2002; 22:91–102. [PubMed: 11900967]
33. Danik SB, Liu F, Zhang J, Suk HJ, Morley GE, Fishman GI, et al. Modulation of cardiac gap junction expression and arrhythmic susceptibility. Circulation research. 2004; 95:1035–1041. [PubMed: 15499029]
34. Chen C, Sun X, Guo P, Dong XY, Sethi P, Cheng X, et al. Human Kruppel-like factor 5 is a target of the E3 ubiquitin ligase WWP1 for proteolysis in epithelial cells. The Journal of biological chemistry. 2005; 280:41553–41561. [PubMed: 16223724]
35. Leithe E, Rivedal E. Ubiquitination and down-regulation of gap junction protein connexin-43 in response to 12-O-tetradecanoylphorbol 13-acetate treatment. The Journal of biological chemistry. 2004; 279:50089–50096. [PubMed: 15371442]
36. Lim KL, Chew KC, Tan JM, Wang C, Chung KK, Zhang Y, et al. Parkin mediates nonclassical, proteasomal-independent ubiquitination of synphilin-1: implications for Lewy body formation. J Neurosci. 2005; 25:2002–2009. [PubMed: 15728840]
37. Sohal DS, Nghiem M, Crackower MA, Witt SA, Kimball TR, Tymitz KM, et al. Temporally regulated and tissue-specific gene manipulations in the adult and embryonic heart using a tamoxifen-inducible Cre protein. Circulation research. 2001; 89:20–25. [PubMed: 11440973]
38. Banerjee I, Fuseler JW, Price RL, Borg TK, Baudino TA. Determination of cell types and numbers during cardiac development in the neonatal and adult rat and mouse. American journal of physiology Heart and circulatory physiology. 2007; 293:H1883–H1891. [PubMed: 17604329]
39. Laird DW. Syndromic and non-syndromic disease-linked Cx43 mutations. FEBS letters. 2014; 588:1339–1348. [PubMed: 24434540]

40. Reaume AG, de Sousa PA, Kulkarni S, Langille BL, Zhu D, Davies TC, et al. Cardiac malformation in neonatal mice lacking connexin43. Science (New York, NY). 1995; 267:1831–1834.
41. Gutstein DE, Morley GE, Tamaddon H, Vaidya D, Schneider MD, Chen J, et al. Conduction slowing and sudden arrhythmic death in mice with cardiac-restricted inactivation of connexin43. Circulation research. 2001; 88:333–339. [PubMed: 11179202]
42. Fromaget C, el Aoumari A, Gros D. Distribution pattern of connexin 43, a gap junctional protein, during the differentiation of mouse heart myocytes. Differentiation; research in biological diversity. 1992; 51:9–20.
43. Fouladkou F, Lu C, Jiang C, Zhou L, She Y, Walls JR, et al. The ubiquitin ligase Nedd4-1 is required for heart development and is a suppressor of thrombospondin-1. The Journal of biological chemistry. 2010; 285:6770–6780. [PubMed: 20026598]
44. Molina-Navarro MM, Trivino JC, Martinez-Dolz L, Lago F, Gonzalez-Juanatey JR, Portoles M, et al. Functional networks of nucleocytoplasmic transport-related genes differentiate ischemic and dilated cardiomyopathies. A new therapeutic opportunity. PLoS One. 2014; 9:e104709. [PubMed: 25137373]
45. Remme CA, Scicluna BP, Verkerk AO, Amin AS, van Brunschot S, Beekman L, et al. Genetically determined differences in sodium current characteristics modulate conduction disease severity in mice with cardiac sodium channelopathy. Circulation research. 2009; 104:1283–1292. [PubMed: 19407241]
46. Scicluna BP, Tanck MW, Remme CA, Beekman L, Coronel R, Wilde AA, et al. Quantitative trait loci for electrocardiographic parameters and arrhythmia in the mouse. Journal of molecular and cellular cardiology. 2011; 50:380–389. [PubMed: 20854825]
47. Yeung B, Ho KC, Yang X. WWP1 E3 ligase targets LATS1 for ubiquitin-mediated degradation in breast cancer cells. PLoS One. 2013; 8:e61027. [PubMed: 23573293]
48. Wackerhage H, Del Re DP, Judson RN, Sudol M, Sadoshima J. The Hippo signal transduction network in skeletal and cardiac muscle. Sci Signal. 2014; 7:re4. [PubMed: 25097035]
49. Del, Re DP.; Yang, Y.; Nakano, N.; Cho, J.; Zhai, P.; Yamamoto, T., et al. Yes-associated protein isoform 1 (Yap1) promotes cardiomyocyte survival and growth to protect against myocardial ischemic injury. The Journal of biological chemistry. 2013; 288:3977–3988. [PubMed: 23275380]
50. Matsui Y, Nakano N, Shao D, Gao S, Luo W, Hong C, et al. Lats2 is a negative regulator of myocyte size in the heart. Circulation research. 2008; 103:1309–1318. [PubMed: 18927464]
51. Smyth JW, Zhang SS, Sanchez JM, Lamouille S, Vogan JM, Hesketh GG, et al. A 14-3-3 mode-1 binding motif initiates gap junction internalization during acute cardiac ischemia. Traffic. 2014; 15:684–699. [PubMed: 24612377]
52. Mund T, Lewis MJ, Maslen S, Pelham HR. Peptide and small molecule inhibitors of HECT-type ubiquitin ligases. Proceedings of the National Academy of Sciences of the United States of America. 2014; 111:16736–16741. [PubMed: 25385595]
53. Fishman GI, Chugh SS, Dimarco JP, Albert CM, Anderson ME, Bonow RO, et al. Sudden cardiac death prediction and prevention: report from a National Heart, Lung, and Blood Institute and Heart Rhythm Society Workshop. Circulation. 2010; 122:2335–2348. [PubMed: 21147730]

## Highlights

- Overexpression of the ubiquitin ligase Wwp1 yields sudden cardiac death in mouse
- Chronic overexpression of Wwp1 promotes left ventricular hypertrophy
- The effects of Wwp1 are cardiomyocyte cell autonomous
- Wwp1 associates with and ubiquitylates connexin 43 contributing to arrhythmogenesis

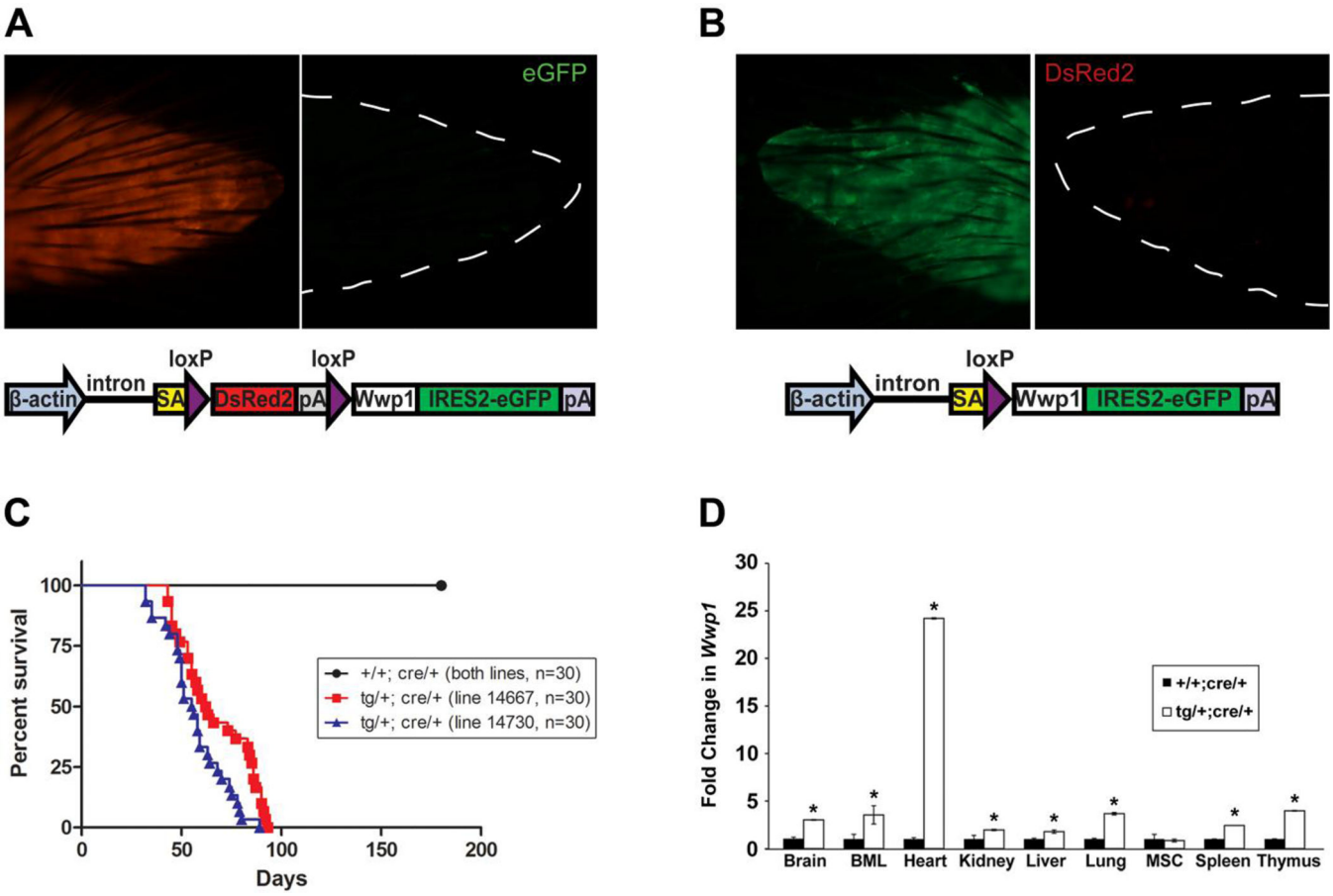


**Fig. 1. Beta-actin driven overexpression of Wwp1 in mice causes sudden death around 8 weeks of age and high levels of expression in the heart**

(**A**) A schematic of the pTraffic construct is depicted. In the inactive state, transgenic mice ubiquitously express DsRed2 resulting in red fluorescence as seen in the representative tail. No fluorescence can be visualized in the green channel. (**B**) Upon crossing to beta-actin cre transgenic mice, the offspring that inherit both the cre transgene as well as the pTraffic-Wwp1 transgene (tg/+; cre/+) ubiquitously overexpress Wwp1 and GFP as pictured in the tail biopsy and no longer express DsRed2. (**C**) A Kaplan-Meier plot summarizing the percent survival for 30 Wwp1 overexpressers (tg/+; cre/+) from two independent founder lines (14667 and 14730) along with 30 wild type littermates (+/+; cre/+) from each line observed over a 180 day period is shown. (**D**) *Wwp1* expression was evaluated in a number of tissues derived from four tg/+; cre/+ animals from each line in comparison to four +/+; cre/+ littermates at 8 weeks of age and normalized to *Gapdh* expression using quantitative real time PCR. SA=splice acceptor, pA=poly-adenylation signal, IRES=internal ribosome entry sequence, BML= bone marrow leukocytes, MSC= mesenchymal stem cells, *p value <0.001.

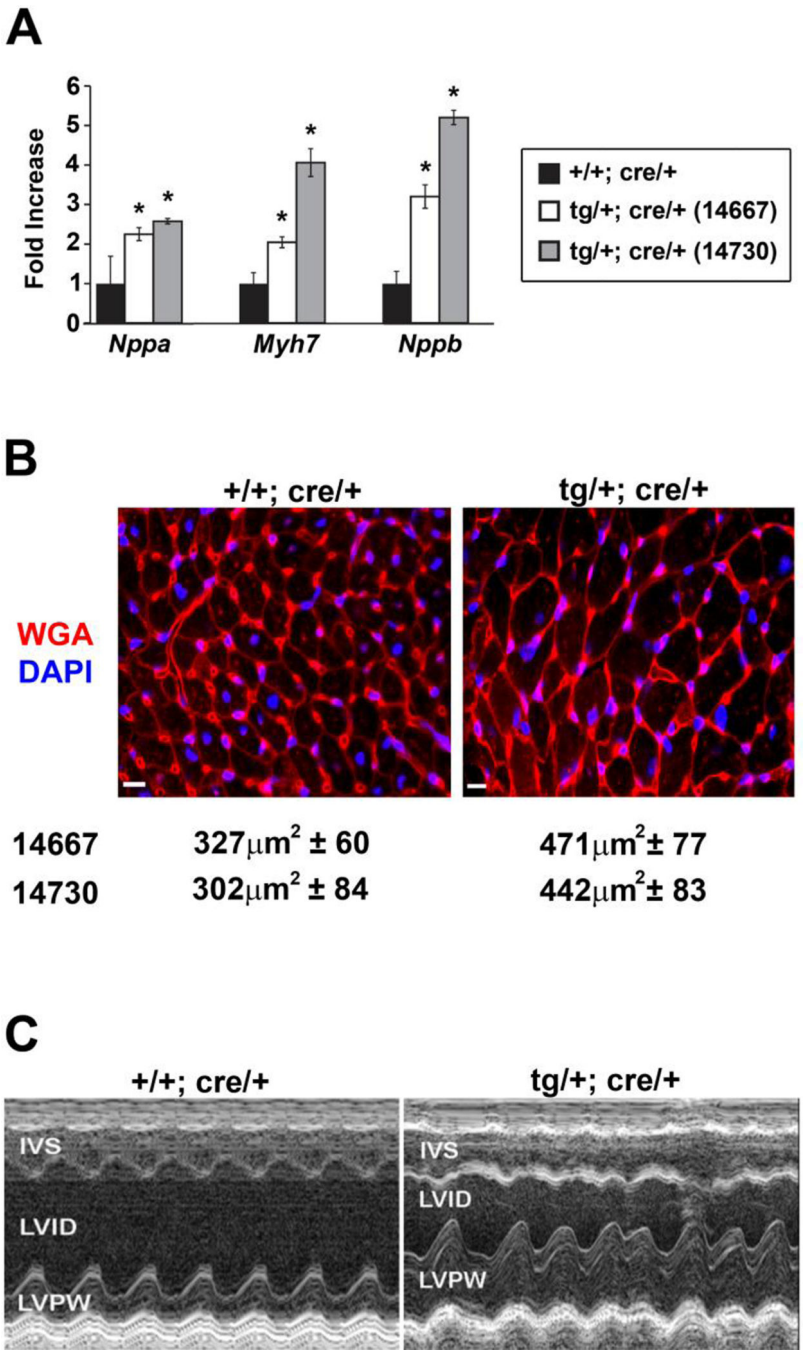


**Fig. 2. Mice that globally overexpress Wwp1 develop LVH**

(**A**) Expression of fetal growth genes associated with cardiomyocyte hypertrophy (*Nppa*, *Myh7*, and *Nppb*) was evaluated in the hearts of 8-week old animals using quantitative real time PCR. Wwp1 overexpressers from both lines (14730 and 14667, n=6) exhibited a significant fold increase in the expression levels of *Nppa*, *Myh7* and *Nppb* when compared to their WT +/+; cre/+ littermates. Mean and standard deviations are shown, *p < 0.01. (**B**) Wheat germ agglutinin (WGA) staining (in red) of cross sections of the left ventricular myocardium derived from 8 week old 14667 (+/+; cre/+ n=4 and tg/+; cre/+ n= 8) and

14730 mice (+/+; cre/+ n=8 and tg/+; cre/+ n= 7) revealed a significant increase in the cardiomyocyte fiber cross sectional surface area in the left ventricle following Wwp1 overexpression in both lines (*p < 0.001). The calculated mean and standard deviation for the cross sectional area for each line and genotype is shown under their respective images. Scale bars = 10μm. (**C**) Representative M-mode echocardiographic traces from 8 week old animals (n=4 of each genotype) reveal thickening of both the interventricular septum (IVS) and the left ventricular posterior wall (LVPW) with a concomitant decrease in the left ventricular internal dimension (LVID). Episodic irregular heartbeats were occasionally noted in the Wwp1 overexpressers but never in WT littermates.

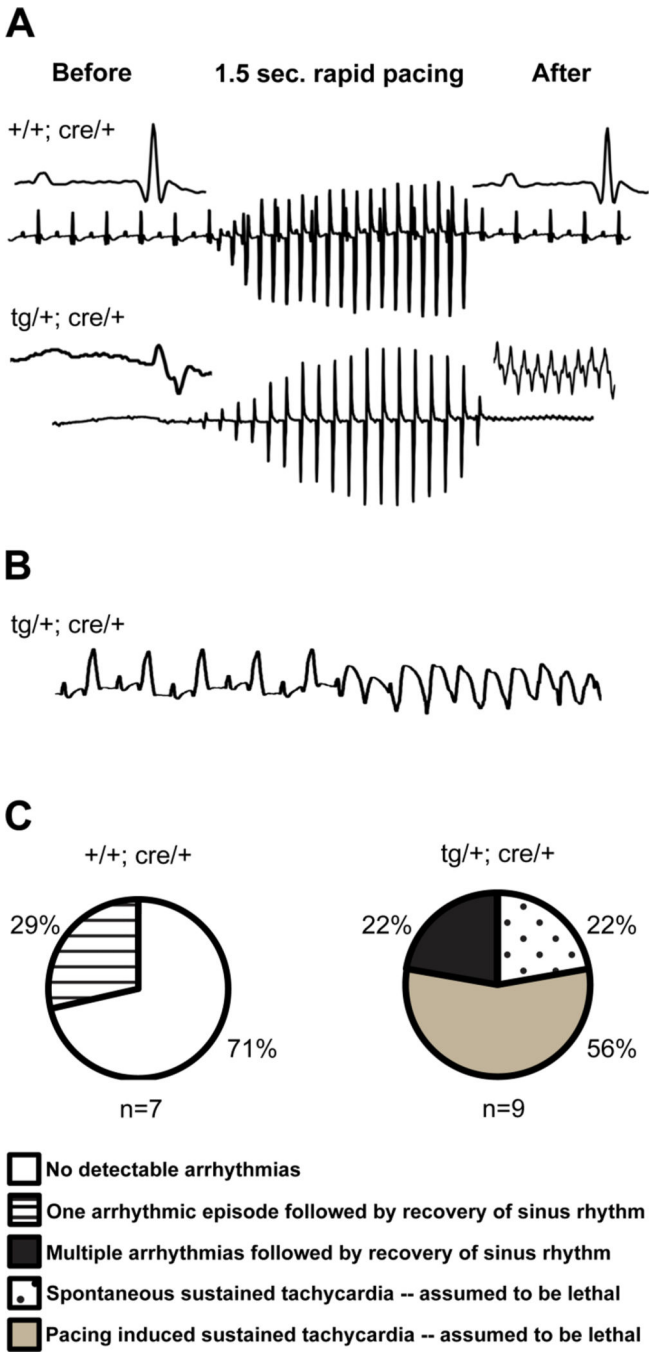


**Fig. 3. Wwp1 overexpressers are highly susceptible to ventricular arrhythmias**

(**A**) Langendorff-perfused hearts from 8 week old Wwp1 overexpressors (tg/+; cre/+, n=9) and from their wild type littermates (+/+; cre/+, n=7) were subjected to an overdrive pacing protocol while electrocardiograms were recorded. Shown are typical electrocardiogram traces from these hearts before and after 1.5 sec rapid pacing. (**B**) In two of the nine hearts derived from Wwp1 overexpressers, spontaneous sustained tachycardia was observed, which was assumed to be lethal *in vivo*. (**C**) A summary of the overdrive pacing findings is presented.

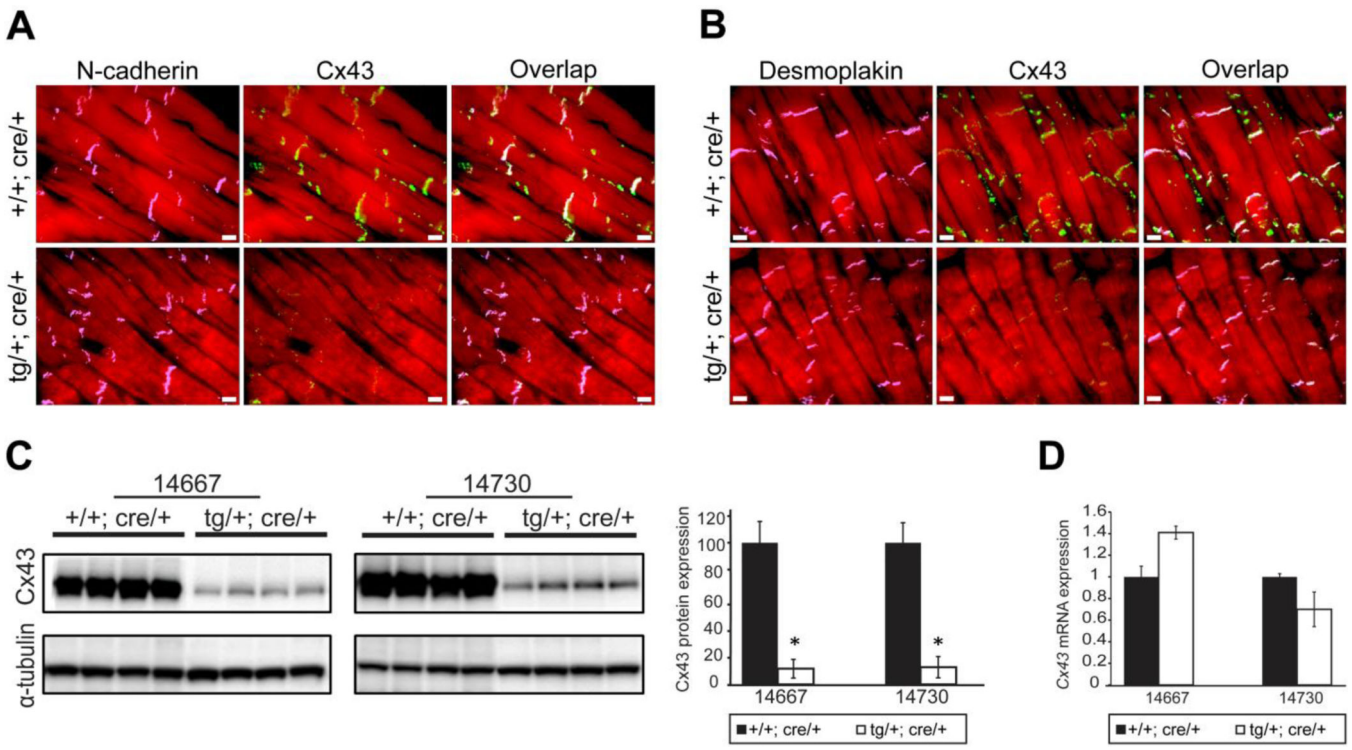


**Fig. 4. Hearts derived from animals overexpressing Wwp1 display Cx43 GJ remodeling**

(**A**) Cryostat heart sections derived from 8 week old tg/+; cre/+ animals (n=4) as well as their +/+; cre/+ littermates (n=4) were immunostained for phalloidin (red), N-cadherin (purple) and Cx43 (green). Animals overexpressing Wwp1 showed generalized mislocalization and greatly reduced amounts of Cx43 while expression of N-cadherin was unaffected. Scale bars = 10μm. (**B**) Frozen sections derived from hearts of 8 week old tg/+; tg/+; cre/+ animals (n=4) or their +/+; cre/+ littermates (n=4) were immunostained for phalloidin (red), desmoplakin (purple) and Cx43 (green). Animals overexpressing Wwp1 showed generalized mislocalization and greatly reduced amounts of Cx43 while expression of desmoplakin was unaffected. Scale bars = 10μm. (**C**) Representative western blot of total heart protein from 8 week old tg/+; cre/+ and +/+; cre/+ mice illustrating a dramatic decrease in Cx43 protein in both the 14667 and 14730 lines. Normalization and quantification of cardiac Cx43 levels in 8 week old mice revealed a statistically significant 88% reduction in Wwp1 overexpressers from the 14667 line and an 87% decrease in the 14730 line relative to their +/+; cre/+ age matched littermate controls (n=5 for each genotype in each line, *$p < 10^{-6}$, error bars represent standard deviations). (**D**) No significant change in *Cx43* mRNA levels in the Wwp1 overexpressers (n=6) relative to their +/+; cre/+ littermates (n=6) was detected by qPCR in both lines. Mean and standard deviation are shown.

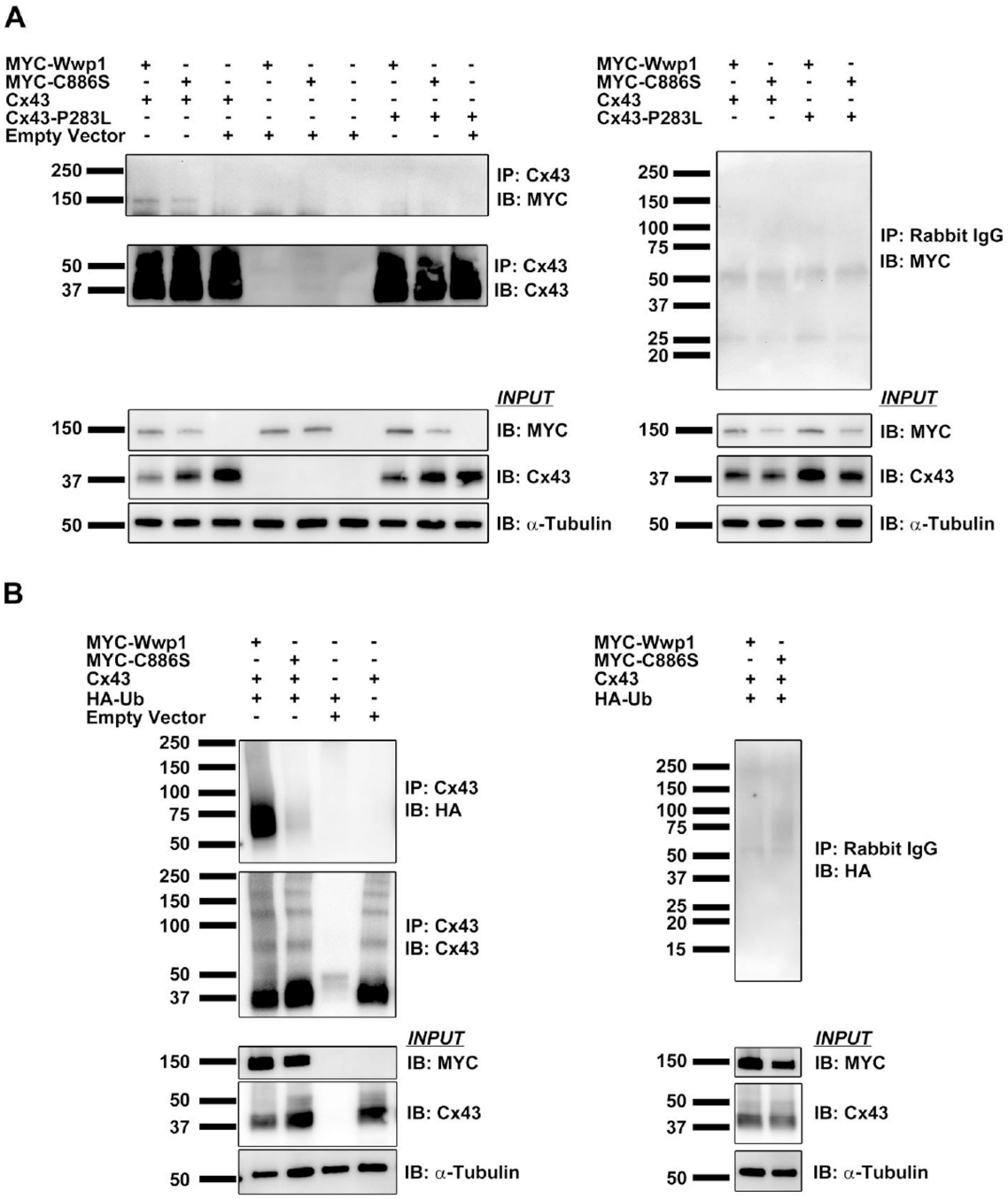


**Fig. 5. Wwp1 co-immunoprecipitates with and ubiquitylates Cx43**

(**A**) Cx43 and either MYC-tagged Wwp1 or a MYC-tagged catalytically inactive form of Wwp1 (MYC-C886S) were transfected into 293T cells with either Cx43 or a PY mutant of Cx43 with the proline residue at position 283 mutated to leucine (Cx43-P283L). Both Wwp1 and Wwp1-C886S could be detected in the immunocomplex with WT Cx43; however the interaction between Cx43 and Wwp1 was abrogated when the Cx43-P283L PY mutant was transfected into the cells. Further, co-expression of WT Wwp1 and WT Cx43 resulted in a decrease in the steady state of Cx43 input. (**B**) To determine whether Wwp1 could

ubiquitylate Cx43, 293T cells were transfected with HA-tagged Ub, Cx43, and either WT or MYC-C886S Wwp1 and, 48h later, were stimulated with PMA for 1hr. Five hours after PMA washout, cells were lysed and subjected to Cx43 immunoprecipitation and then the protein extract was immunoblotted with an anti-HA antibody to detect ubiquitylation. While WT Wwp1 mediated robust ubiquitylation of Cx43, the Wwp1-C886S mutant could not. This was also reflected in the decreased Cx43 detected in the input of cells transfected with WT Wwp1 and Cx43.

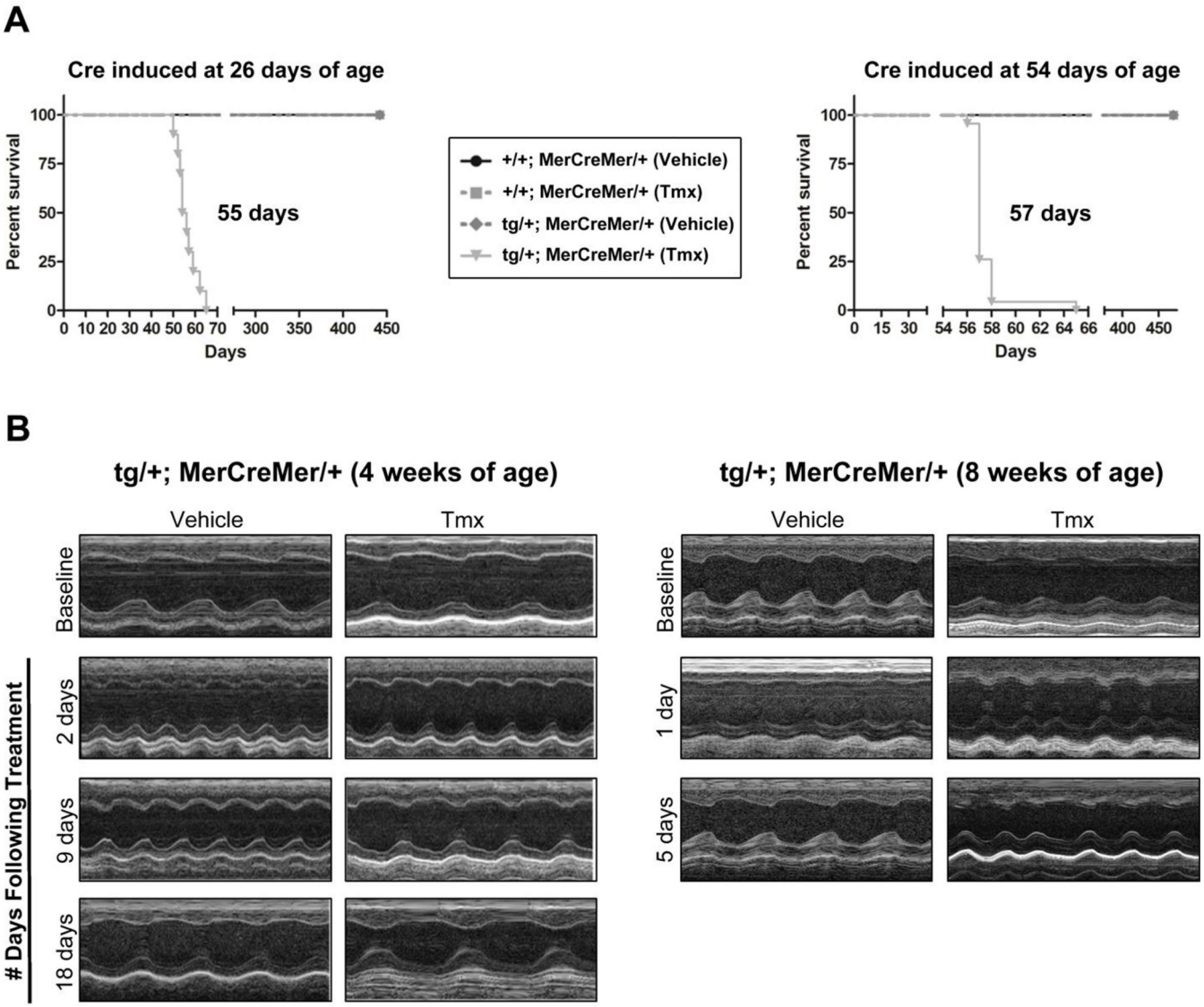


**Fig. 6. Cardiomyocyte-specific overexpression of Wwp1 yields sudden death and age-dependent LVH**

(**A**) The pTraffic-Wwp1 transgenic mice were mated to mice homozygous for a tamoxifen (Tmx)-inducible cre under the control of the cardiomyocyte-specific alpha -myosin heavy chain promoter (MerCreMer), yielding offspring that carried just the cre construct (+/+; MerCreMer/+) or animals that carried both the pTraffic-Wwp1 and the MerCreMer transgenes (tg/+; MerCreMer/+). Only tg/+; MerCreMer/+ that received two consecutive intraperitoneal injections of Tmx (40 mg/kg/day) beginning at either 26 days of age (n=10) or 54 days of age (n=17) exhibited a sudden cardiac death phenotype around 8 weeks of age (55 and 57 days, respectively). All the vehicle-treated mice (+/+; MerCreMer/+, n=10 for each timepoint or tg/+; MerCreMer/+, n=10 and n=15 for the earlier and later timepoint, respectively) as well as the Tmx-treated +/+; MerCreMer/+ mice (n= 10 for each start point) lived a normal life span as summarized in the Kaplan-Meier plots. (**B**) Serial transthoracic echocardiographs were obtained from tg/+; MerCreMer mice treated with vehicle or Tmx

beginning at 26 days of age (n=3 for each, panels on the left) or at 54 days of age (n=3 for each, panels on the right). Representative M-mode traces illustrate the LVH that developed in Tmx-treated animals 18 days following cre induction but not in vehicle-treated littermates while those tg/+; MerCreMer mice that were administered Tmx (n=3) or vehicle (n=3) beginning at 54 days of age show episodic irregular heartbeats without LVH.

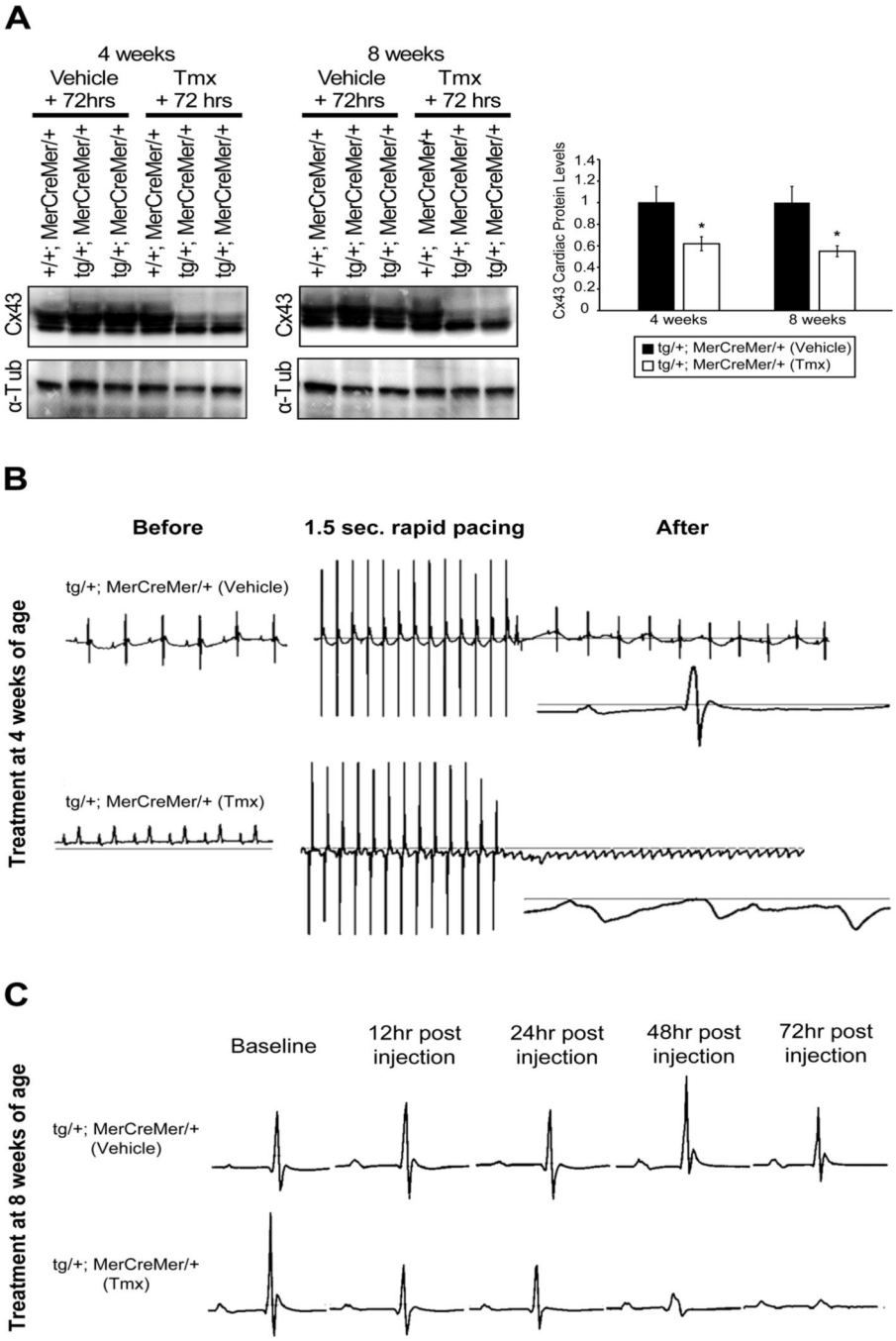


**Fig. 7. Cardiomyocyte-specific overexpression of Wwp1 results in a rapid decrease in Cx43 protein levels, EKG abnormalities and high susceptibility to cardiac arrhythmia**

(**A**) Wwp1 was overexpressed in the cardiomyocytes of tg/+; MerCreMer/+ mice beginning at 26 or 54 days of age via Tmx injection. Total protein was harvested from hearts 72 hours later and Cx43 levels were determined by Western blotting and densitometry. This analysis revealed a 38% decrease in normalized total cardiac Cx43 protein levels in animals injected at 26 days of age and a 45% decrease in normalized total cardiac Cx43 protein levels in animals treated with Tmx beginning at 54 days of age as compared to age-matched, vehicle-

injected tg/+; MerCreMer/+ controls (n=3 for each genotype, treatment, and age). (**B**) Twenty-six day old tg/+; MerCreMer/+ mice were either vehicle- or Tmx-injected (n=3 for each treatment). One week later, hearts from these animals were Langendorff-perfused and subjected to an overdrive pacing protocol while electrocardiograms were recorded. Shown are typical traces from these hearts before and after 1.5 sec rapid pacing. Abnormal baseline waveforms were only noted in the hearts isolated from the Tmx-induced Wwp1 overexpressers. While all vehicle treated hearts quickly recovered sinus rhythm following pacing during this protocol, those hearts with cardiomyocyte specific overexpression of Wwp1 derived from the Tmx-treated tg/+; MerCreMer/+ mice displayed ventricular arrhythmias. (**C**) Tg/+; MerCreMer/+ mice were injected with either vehicle (n=4) or Tmx (n=4) at 54 days of age and serial electrocardiograms were recorded in this cohort of animals at 12, 24, 48 and 72 hours following injections. Cardiomyocyte-specific overexpression of Wwp1 induced by Tmx caused a significant decrease in the amplitude of the QRS wave at 12 and 24 hours post injection followed by further reduction in the QRS amplitude as well as prolongation of the QT interval at 48 and 72 hours following induction. The vehicle-treated tg/+; MerCreMer/+ mice, on the other hand, showed no significant changes in their EKG traces at any of the time points following injection when compared to the baseline measurement. *$p < 0.01$